# PID Control in a Toy Bio-economic Model

**©Alexander V. RYZHENKOV**

Economic Faculty
Novosibirsk State University
1 Pirogov street Novosibirsk 630090 Russia
Institute of Economics and Industrial Engineering
Siberian Branch of Russian Academy of Sciences
17 Academician Lavrentiev Avenue Novosibirsk 630090 Russia
E-mail address: ryzhenko@ieie.nsc.ru

## *Abstract*

The mathematic control theory is applied to the development of modifications of the Schaefer fishery model. The key variables are the stock of the bio-resource, its natural net change, as well as the Man harvesting activity. The global and local analysis reveals quantitative and qualitative characteristics of closed loop control in a heuristic harvesting control rule in a two-dimensional model. Deeper analyses refine and generalize this rule in a three-dimensional model. The synthetic proportional, integral and derivative (PID) control together with parametric policy optimization maintains a robust harvesting control rule. Still unwarranted strength of integral control is destabilizing and can bring about Andronov – Hopf bifurcation in a local vicinity of a non-trivial stationary state.

Key words: renewable resource, maximum sustainable yield, harvesting effort, PID control, optimization, Andronov – Hopf bifurcation

## *1 Introduction*

As well established by system dynamics research over decades, reserves of fish and other resources of flora and fauna, due to their natural reproductive capacity, can grow, contributing to the preservation and increase of natural capital [1, 2]. However, according to the World Bank experts [3, 4], a decrease in the biomass of global fish stocks, as a result of their excessive catch, created a threat to sustainable fishing.

Unsustainable management of renewable resources can lead to their permanent depletion in much the same way as the finite extraction of nonrenewable resources. Stagnant or declining (even slightly) catches can accompany a long-term decline in fish stock. If left unchecked, harvesting could destroy the fisheries that would become biologically or commercially extinct over time.

Global marine fisheries are in crisis. The proportion of fisheries that are fully fished, overfished, depleted, or recovering from overfishing increased from just over 60 percent in the mid-1970s to about 75 percent in 2005 and to almost 90 percent in 2013." [4, p. 1]. These observations have been later revised in FAO (2022) [5, p. xvi]: "Fishery resources continue to decline due to overfishing, pollution, poor management and other factors, but the number of landings from biologically sustainable stocks is on the rise. The fraction of fishery stocks within biologically sustainable levels decreased to 64.6 percent in 2019, 1.2 percent lower than in 2017. However, 82.5 percent of the 2019 landings were from biologically sustainable stocks, a 3.8 percent improvement from 2017."

In spite of the given FAO (2022) optimistic assessment of the rising number of landings from biologically sustainable stocks, there is still an urgent need for a transition to fundamentally more favourable natural-anthropogenic regimes [ibid.]: “Effective fisheries management has been proven to successfully rebuild stocks and increase catches within ecosystem boundaries. Improving global fisheries management remains crucial to restore ecosystems to a healthy and productive state and protect the long-term supply of aquatic foods.”

A transition to fundamentally more favourable natural-anthropogenic regimes should be based on in-depth studies of contrasting regimes of ecological and economic interaction based on system dynamics models, starting with engaging ones such as Fish Banks Game developed by D. Meadows and his colleagues reflected in [2]. A great constructive role in clarification of such models and in their further development belongs to the mathematical control theory [6] with strong roots in the mathematical analysis and the theory of differential equations.

According to the control theory, open-loop control is completely determined at the initial instant $t_0$; here, the integration of the equation (or equations) of motion for fixed initial conditions defines the phase trajectory $x(t)$ of the states of the system [7]. Closed-loop control (with feedback) assumes the definition of control as a function of phase coordinates and time [ibid.]. These concepts have wide theoretical and applied significance for the economic theory and the economic practice.

To simplify exposition of economics of renewable resources we will keep in mind their rich diversity and consider non-farming fish as their representative. Peculiarities of specific types of these resources are not considered on this stage of investigation.

Then according to existing conventions, biomass is total amount of fish resources, biomass net change is due to natural processes and harvesting by Man. Hereby harvest equals yearly catch.

A time derivative of a variable, say, $x$ is indicated by a dot directly above it ($\dot{x} = \frac{\partial x}{\partial t}$), whereas its growth rate is similarly marked by a hat $\hat{x} = \frac{\dot{x}}{x} = \frac{1}{x}\frac{\partial x}{\partial t}$. Of course, growth rate $\hat{x}$ is the same as the time derivative of $\ln(x)$. Table 1 lists model variables and their units of measurement. It may be a prompt on variables of differential equations below.

Table 1. The main variables of simplified biomass models

| Variable | Notation | Measurement unit |
|---|---|---|
| Effort | $e$ | fraction of unit |
| Expected effort | $y$ | fraction of unit |
| Catch | $c$ | fish/year |
| Fish stock (biomass) | $x$ | fish |
| Carrying capacity | $1/\alpha$ | fish |
| Birth rate | $\beta x$ | fish/year |
| Death rate | $-\beta\alpha x^2$ | fish/year |
| Net change of fish stock | $\dot{x}$ | fish/year |
| The growth rate of fish stock | $\hat{x}$ | 1/year |

The reader sees that global marine fish stock is considered as a scalar. This permits an application of a single equation technique akin to methods developed in the research on mineral resources and proved stocks (see references and critique in [8–10]).

Sections 2, 3 and 4 have benefited from [11]; these sections are devoted to maximal sustainable yield-centred stabilization in two- and three-dimensional predator-prey models that enhance sustainable harvesting thanks to combined control over the effort, catch, and fish stock (at first, proportional and derivative control, secondly, proportional, derivative and integral control).

Section 2 starts from the textbook Verhulst model denoted as M-1. The author offers a simplified two-dimensional Verhulst – Schaefer model [12] extended by a heuristic harvesting control rule from [13]. The stock-and-flow structure of this predator-prey model named M-2 is revealed. Proportional and derivative control is elaborated as a combination of rather reliable first-order feedback loops in the extensive form of this model. It is demonstrated that the dynamics in this model linearized in the neighbourhood of its hyperbolic stationary state are locally asymptotically stable (LAS). The non-trivial stationary state is also LAS in M-2 as the non-linear system. The books [14, 15] are the sources of knowledge (among others) on the Routh – Hurwitz stability criterion and on Andronov – Hopf bifurcation applied in this paper.

Section 3 refines proportional and derivative control elements and adds the remaining element of integral control that maintains sustainable harvesting stronger in a three-dimensional predator-prey model tagged as S-2. The stock-and-flow diagrams (SFDs) for the extensive and intensive forms of this model are exposed. Under the restrictions on three key parameters the dynamics of the system linearized in the neighbourhood of its hyperbolic stationary state are LAS. It is shown that this is true in the non-linear S-2 as well. An elaborated form of PID control generalizes the previous forms of control considered in this paper earlier.

Section 4 compares the heuristic HCR in M-2 with the HCR based on the proposed PID control in S-2. It is possible for the PID control in S-2, as demonstrated, to match the heuristic HCR in M-2 even with an inactive integral element. On the other hand, it is not always possible to match the PID control in S-2 through the heuristic HCR in M-2. Therefore the PID control in S-2 is a reasonable generalization of the heuristic HCR in M-2 that can be potentially more efficient in the social management of bio-economic processes.

## *2 Simplified Verhulst – Schaefer two-dimensional model M-2 including the heuristic harvesting control rule (HCR)*

### 2.1 Verhulst textbook model M-1

The logistic equation, also known as the Verhulst equation (named after the Belgian mathematician), originally appeared when considering the model of wild population growth. Denoting by $x$ the population size, by $t \geq 0$ time, the model can be represented by a non-linear autonomous differential equation

$$\dot{x} = \phi(x) = \beta x(1-\alpha x), \tag{1}$$

where parameter $\beta$ characterizes the potential rate of growth (multiplication) in the absence of intraspecific competition, and $\alpha$ is the reciprocal of the supporting capacity of the environment (that is, the inverse of the maximum possible population size).

Fish hatch (give birth), grow to maturity, lay eggs and die. The fish death rate is the number of fish per year that die from causes other than fish harvesting. Factors of fish population simple growth are depicted on Figure 1. The abbreviation SFD means stock-and-flow diagram through this paper.

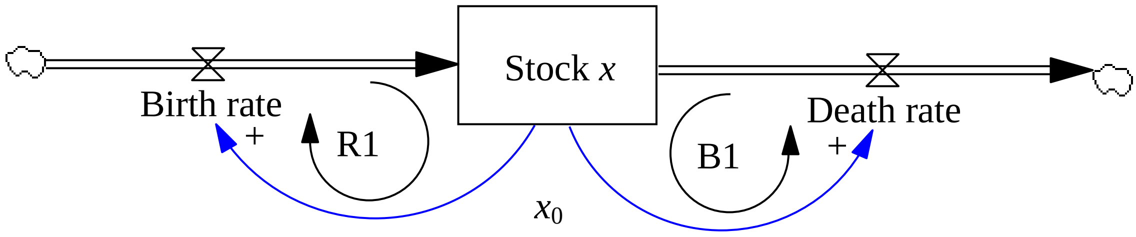


Figure 1 – The SFD of M-1

The initial assumptions for the derivation of the equation when considering population dynamics are as follows: the rate of reproduction of the population is proportional to its current level; the second term of the equation reflects intraspecific competition for resources, which limits the growth of the population, or, in plain words, the death rate increases as crowding increases.

The derivative of the natural net change is defined as

$$\phi_x{}' = \beta - 2\alpha\beta x. \qquad (2)$$

When $\phi_x{}' = 0$, net increment $\phi(x)$ is maximal for $x_s = 1/(2\alpha)$. This property maintains the maximal sustainable yield below.

The stationary states are found from the condition that the right-hand side of (1) is equal to zero. They differ qualitatively and quantitatively.

On the one hand, $x_1 = 1/\alpha$ is an asymptotically stable node, since $\phi_x{}'(x_1) = -\beta < 0$, on the other hand, $x_2 = 0$ – unstable node, as $\phi_x{}'(x_2) = \beta > 0$.

The population growth is S-shaped. Neither open nor closed loop control of the wild population by Man is active. The size of the population tends to dynamic equilibrium at the maximum number that can sustain most of random external shocks except huge calamities. M-1 is structurally stable. Without huge loss of generality, let $\alpha = 1$ and $\beta = 1$ [16, pp. 98–99].

## 2.2 The heuristic Harvesting Control Rule in Verhulst – Schaefer two-dimensional model

The model [12] supplements the assumptions of the logistic growth of biomass by the assumption that human fishing activities reduce the increase in the fish population by catch amount $c$ that linearly depends on the effort $e$:

$$\dot{x} = f(x) = x(1 - x) - c, \qquad (3)$$

where $c = he$, $h$ = const = 0.25.

In other models catch $c$ depends positively on stock $x$ raised to a deliberate positive power additionally [10]. The fish stock that gives the maximum sustainable yield ($c_s = 0.25$) at fitting sustainable effort ($e_s = 1$) represents the desired sustainable level ($x_s = 0.5$) in agreement with (2).

The harvesting control rule (HCR) has been formulated in [13, p. 152] "as an anchoring and adjustment heuristic, consistent with what has been suggested in studies of judgements under uncertainty." Therefore the term heuristic HCR is used through the rest of this paper.

The subjects manage a renewable resource, a reindeer rangeland. The most important dynamic factor for reindeer management is lichen, the plant providing the main source of winter fodder for the reindeer.

The present paper proposes the following concretization of the heuristic HCR for the Verhulst – Schaefer two-dimensional model. Fish stock $x$ takes place of lichen, Man's effort $e$ (desired and realised) plays the role of reindeers. The effort results in catch of the fish as an important and valuable source of the human nutrition. The anchor is traditional or expected fish stock $y$. The adjustment is directed to closing the gap between desired fish stock $x_s$ and actual stock $x$.

The Verhulst – Schaefer two-dimensional model with the heuristic HCR is denoted as M-2. Figure 2 and Table 2 shed light on this HCR as a promising leverage thereby.

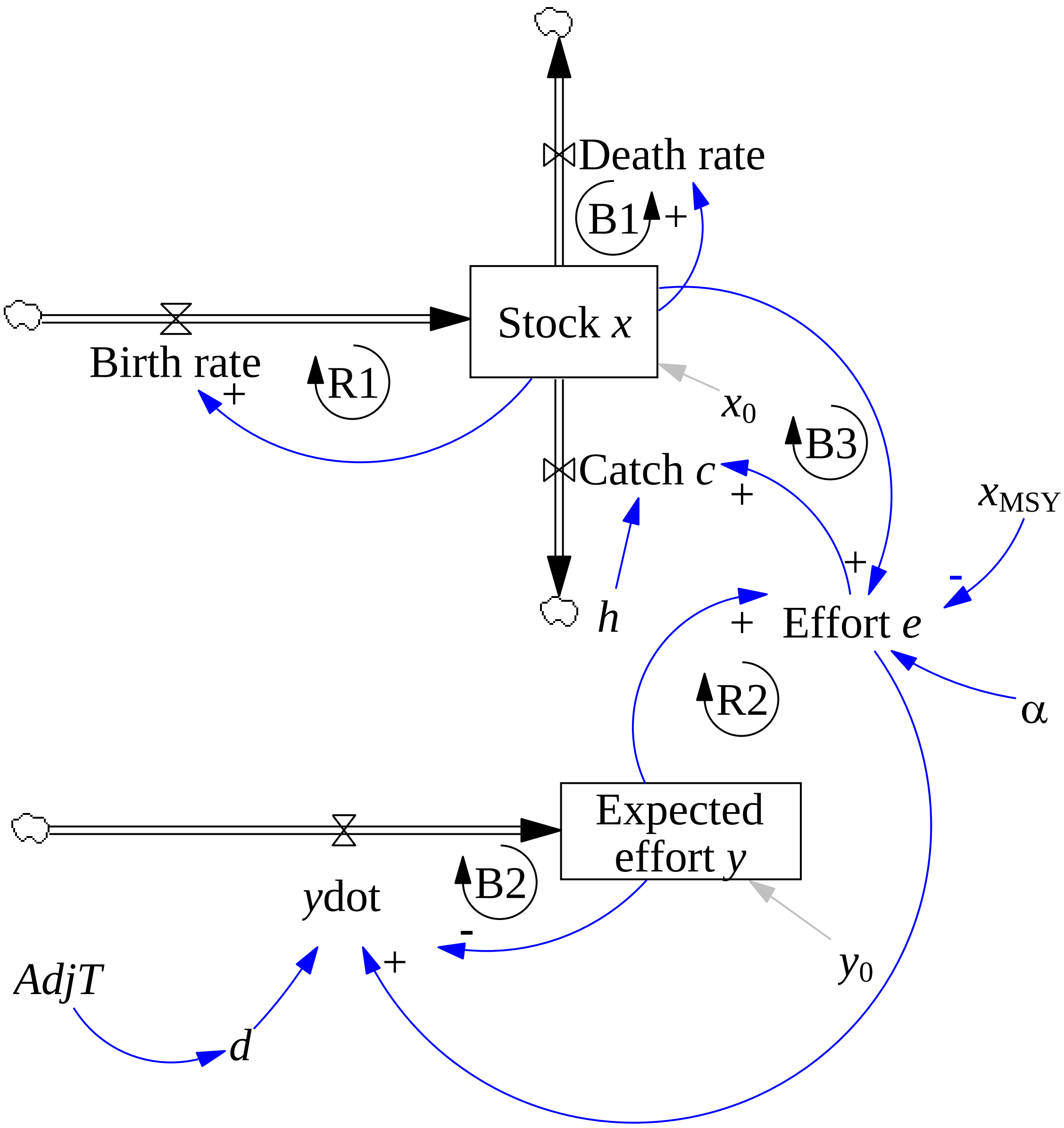


Figure 2 – The SFD of M-2 with the heuristic HCR

Table 2. Five feedback loops in the extensive form of M-2 with the heuristic HCR

| No | Order, sign | Loop |
|---|---|---|
| B1 | 1, - | Stock $x \xrightarrow{+}$ Death rate $\xrightarrow{-}$ |
| R1 | 1, + | Stock $x \xrightarrow{+}$ Birth rate $\xrightarrow{+}$ |
| B3 | 1, - | Stock $x \xrightarrow{+}$ Effort $e \xrightarrow{+}$ Catch $c \xrightarrow{-}$ |
| B2 | 1, - | Expected effort $y \xrightarrow{-}$ Net change of $y$ ($y$dot) |
| R2 | 1, + | Expected effort $y \xrightarrow{+}$ Effort $e \xrightarrow{+}$ Net change of $y$ ($y$dot) |

There are surprisingly only the 1st order feedback loops in this extensive form of M-2: among the total number of five, there are two positive and three negative loops that can be an incredibly useful arsenal for badly needed enhancement of social control over the depleted bio-stock. This HCR is metaphorically intended to empower the Man whose hands hold the bull's horns for taming the beast.

The adjustment of effort $e$ is set relative to expected effort $y$ non-linearly:

$$e = y - \frac{\alpha(x_S - x)}{x_S} y =$$

$$= y\left[(1-\alpha) + \alpha\frac{x}{x_S}\right]. \tag{4}$$

There is positive dependence of $e$ on $y$ and on $x$. For $e_0$ given historically an initial expected effort is defined in agreement with (4) as

$$y_0 = \frac{e_0}{1-\alpha \;+\; \alpha x_0 / x_S} =$$

$$= e_0 \frac{x_S}{\alpha x_0 \;+ (1-\alpha) x_S}\,. \tag{5}$$

Clearly, $y_0 > e_0$ if $x_0 < x_S$ and $y_0 \le e_0$ if $x_0 \ge x_S$ .

Lower magnitudes of α will lead to weaker adjustments and vice versa. Excessively weak adjustment of a depleted fish stock can result in undesirable collapse of the bio-resource.

Expected effort $y$ is updated by recent experiences. A policy is described by the first order information delay:

$$\dot{y} = d(e-y) = d\left[ y(1-\alpha) + \alpha y \frac{x}{x_S} - y \right] =$$

$$= d\alpha y \frac{x - x_S}{x_S}, \tag{6}$$

hereby, in tendency, expected effort $y$ (stock) smooths effort $e$ (auxiliary), $e$ leads $y$.

Equation (6) substitutes a similar equation for a traditional herd size in the discrete time model with a time step of one year for the applied *AdjT* = 10 (years) in [13, p. 152]. Thereby the traditional herd size is smoothed and delayed transformation of the herd size itself. However, the model, simulated with a time step of 1, can still be thought of as a continuous model, since the implicit time constants are much longer than 1 [13, p. 158]. The time constants in M-2 for fisheries could be substantially lower than $AdjT$ = 10. This motivates transition to continuous ordinary differential equations (ODEs) with a substantially shorter time step in integration of these equations in the present paper.

The intensive form of M-2 consists of two ODEs (3) and (6). The initial condition is one of overfishing, with fish stock $x_0 < x_s$ and excessively high expected effort $y_0 > y_s$ for the historically given effort $e_0$ that is also excessive for the given fish stock $x_0$.

For this system, i.e., ODEs (3) and (6), the Jacoby matrix is defined as

$$J_{\text{M-2}} = \begin{array}{|c|c|} \hline 1 - 2x - \frac{\alpha}{2} y & -\frac{1-\alpha}{4} - 0.5\alpha x \\ \hline 2d\alpha y & d\alpha \frac{x - x_s}{x_s} \\ \hline \end{array} . \tag{7}$$

In the intensive form of M-2, expected effort $y$ is the predator, fish stock $x$ is the prey. Intraspecific co-operation of preys takes place if $1 - 2x > \frac{\alpha}{2} y$. Similarly, intraspecific co-operation of predators takes plays if $x > x_s$. Preys compete with each other if $1 - 2x < \frac{\alpha}{2} y$. A neutral case is for $1 - 2x = \frac{\alpha}{2} y$. Similarly, predators compete with each other if $x < x_s$. A neutral case here is for $x = x_s = 0.5$.

Therefore there five feedback loops for this intensive form of M-2 revealed thanks to the Jacoby matrix $J_{\text{M-2}}$: two positive 1$^{st}$ order loops, two negative 1$^{st}$ order loops and single negative 2$^{nd}$ order loop (Table 3). This constellation is simplified in the vicinity of the stationary state below (Table 4).

Table 3. Feedback loops in the intensive form of M-2 for $0 < \alpha \le 1$

| No | Order, sign | Loop |
|---|---|---|
| 1 | 1, + | $x \xrightarrow{+} \dot{x}$ for $1 - 2x > 0.5\alpha y$ |
| 2 | 1, - | $x \xrightarrow{-} \dot{x}$ for $1 - 2x < 0.5\alpha y$ |
| 3 | 1, + | $y \xrightarrow{+} \dot{y}$ if $x > x_s$ |
| 4 | 1, - | $y \xrightarrow{-} \dot{y}$ if $x < x_s$ |
| 5 | 2, - | $x \xrightarrow{+} \dot{y} \longrightarrow y \xrightarrow{-} \dot{x}$ |

The above system, consisting of ODEs (3) and (6), has the non-trivial stationary state:

$$E_s = (x_s, y_s), \tag{8}$$

where $x_s = 0.5$, $y_s = e_s = 1$.

Additionally this system has two trivial stationary states (0, 0) and (1, 0) that are unstable and repelling in relevant cases, whereas the non-trivial stationary state serves as the point attractor (node or focus). The stability analyses of these two trivial stationary states on the phase plane are omitted for brevity.

For stationary state ($x_s$, $y_s$) of this system the Jacobi matrix, enabling linearization of M-1 in vicinity of (8), is defined as

$$J^*_{M-2} = \begin{vmatrix} -0.5\alpha & -0.25 \\ 2d\alpha & 0 \end{vmatrix} . \tag{9}$$

There is more certainty in relations near this state: preys compete with each other, predators do not. These competitive relations within fish stock $x$ as well as between fish stock and expected effort $y$ are stabilizing (Table 4).

Table 4. Intensive FB loops for vicinity of stationary state $E_s$ in the compact system

| No. | Order, sign | Loop |
|---|---|---|
| 1 | 1, - | $x \xrightarrow{-} \dot{x}$ |
| 2 | 2, - | $x \xrightarrow{+} \dot{y} \longrightarrow y \xrightarrow{-} \dot{x}$ |

**Proposition 1** The dynamics of the system (3) and (6) linearized in the neighbourhood of its hyperbolic stationary state $E_s$ (8) are locally asymptotically stable (LAS). Then stationary state $E_s$ is also LAS in the non-linear system (3) and (6).

***Proof of Proposition 1*** For gaining additional information consider a corresponding characteristic equation

$$\lambda^2 + m\lambda + n = 0. \tag{10}$$

Notice $m = -Trace(J^*_{M-2})$ and $n = \left|J^*_{M-2}\right|$. According to the Routh–Hurwitz criterion, if $Trace(J^*_{M-2})$ is negative and its determinant $\left|J^*_{M-2}\right|$ is positive, stationary state $E_s$ is LAS – see [14, p. 239].

In the present model, the first and second inequalities are satisfied:

$$\left|J^*_{M-2}\right| = 0.5d\alpha > 0 \tag{11}$$

and

$$Trace(J^*_{M-2}) = -0.5\alpha < 0. \tag{12}$$

The characteristic equation (10) has two negative real roots if $\alpha - 8d \geq 0$:

$$\lambda_{1,2} = \frac{1}{4}\left[-\alpha \pm \sqrt{\alpha(\alpha - 8d)}\right] < 0, \tag{13}$$

particularly,

$$\lambda_1 = \lambda_2 = -0.25\alpha \tag{14}$$

if $d = \dfrac{\alpha}{8}$.

Equation (10) has two complex-conjugate roots with negative real part $\mathrm{Re}(\lambda_1) = \mathrm{Re}(\lambda_2)$ if $\alpha - 8d < 0$:

$$\lambda_{1,2} = -0.25\alpha \pm 0.25i\sqrt{-\alpha(\alpha - 8d)}\,. \qquad (15)$$

A period for converging cycles for LAS focus $E_s$ is

$$T_c \approx \frac{8\pi}{\sqrt{-\alpha(\alpha - 8d)}}. \qquad (16)$$

In both cases (two negative real roots or complex-conjugate roots with negative real part) the linearized system is hyperbolic. This confirms LAS of $E_s$ in the non-linear system (3) and (6) as well. Table 5 and Figure 3 reflect the dependence of the roots of characteristic equation (10) on magnitude of parameter $d$ for the given magnitude of parameter $\alpha$. Policy optimization through the two parameters ($\alpha$ and $d$) tuning in M-2 is considered in Section 4.

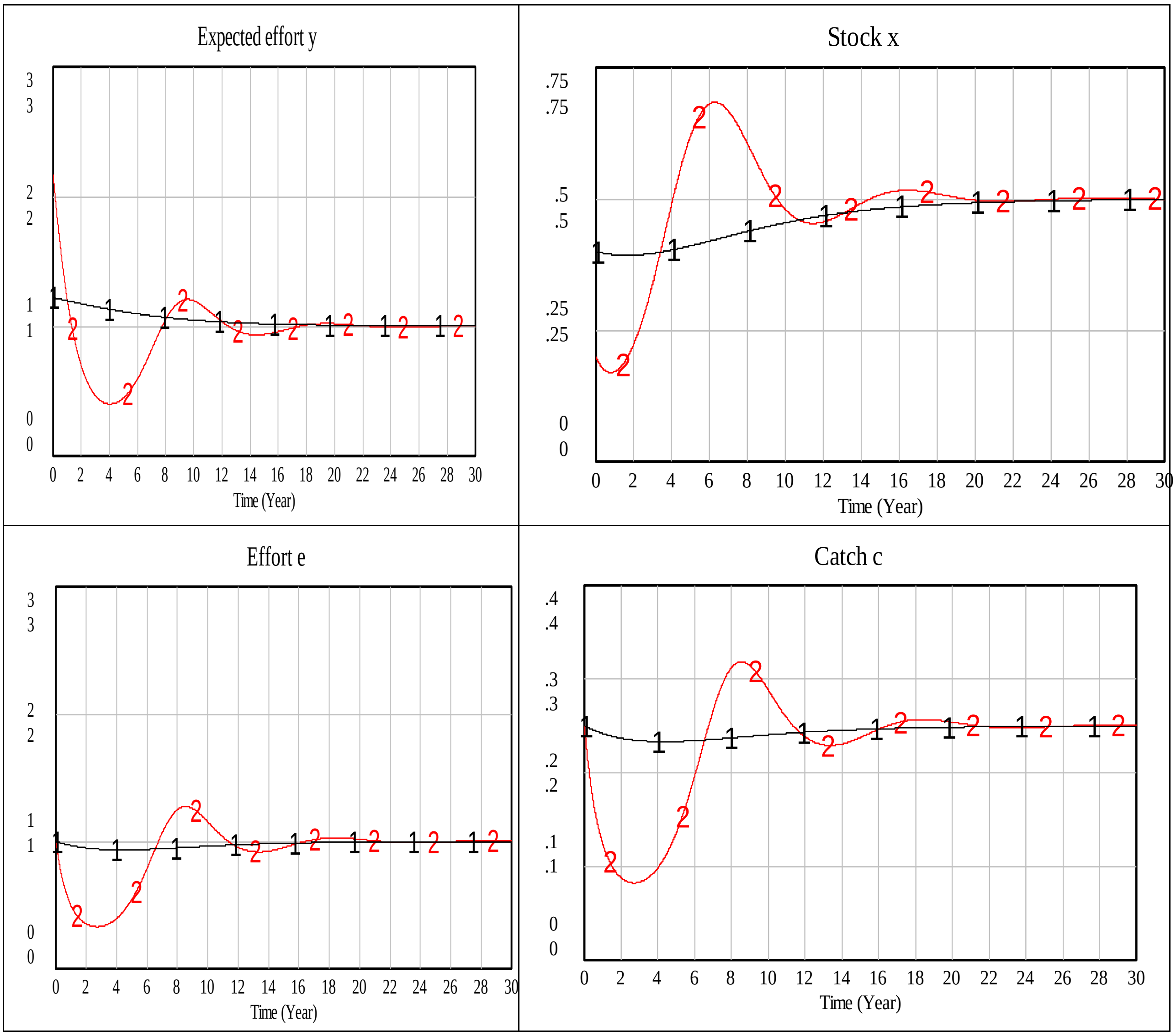


Figure 3 – Examples of LAS node $E_s$ (8) for $AdjT$ = 10, $d$ = 0.1, $x_0$ = 0.4 and LAS focus $E_s$ (8) for $AdjT$ = 1, $d$ = 1, $x_0$ = 0.2

Table 5. Roots of characteristic equation (10) for $\alpha = 0.9$ depending on parameter $d$

| Root | LAS node $E_s$ for $d = 0.1$ | LAS node $E_s$ for $d = 0.1125$ | LAS focus $E_s$ for $d = 1$ |
|---|---|---|---|
| $\lambda_1$ | –0.15 | –0.225 | - |
| $\lambda_2$ | –0.3 | –0.225 | - |
| $\mathrm{Re}(\lambda_1)$ | - | - | –0.225 |
| $\mathrm{Im}(\lambda_1)$ | - | - | $0.632i$ |
| $\mathrm{Re}(\lambda_2)$ | - | - | –0.225 |
| $\mathrm{Im}(\lambda_2)$ | - | - | $-0.632i$ |
| Period $T_c$ | - | - | 9.942 y. |

Catch $c$ remains positive even for initially strongly depleted stock ($x_0 = 0.2$) for $\alpha$ sufficiently high (particularly, $\alpha = 0.9$). Quite differently, unsound control with $\alpha = 0.001$ results in extinction of the fish within 10 years for $AdjT = 10$, $d = 0.1$, $e_0 = 1$ and $x_0 = 0.4$.

## 3 PID control in a three-dimensional bio-economic model

A proportional–integral–derivative controller (PID controller) continuously calculates an error value as the difference between a target and a measured process variable and applies a correction based on proportional, integral, and derivative terms (denoted P, I, and D respectively), hence the name [11, 17].

### 3.1 Additional dimension of the controlled system through integral control in S-2

Figure 4 and Table 6 present the stock and flow diagram of the extensive form of S-2, whereby: a total number of feedback loops – 6, among them: 1st order – 2 (negative and *positive*), 2nd order – 3 (2 – negative, 1 – *positive*), 3rd order – 1 (negative).

*Net change edot P* stands for the element of proportional control, *Net change edot I* expresses the element of integral control; finally, *Net change edot D* relates to the element of derivative control. The sum of these three elements equals the derivative of effort $e$ with respect to time. Discrepancy $D$ (as stock) integrates the instant difference between current stock $x$ and the target stock $x_s = x_{\mathrm{MSY}}$ that enables maximal sustainable yield.

The reader may notice that capital letter with italics $D$ stands for a new phase variable in S-2 that differs from the parameter denoted as small letter with italics $d$. Capital letter without italics D in the abbreviation PID relates to the element of derivative control.

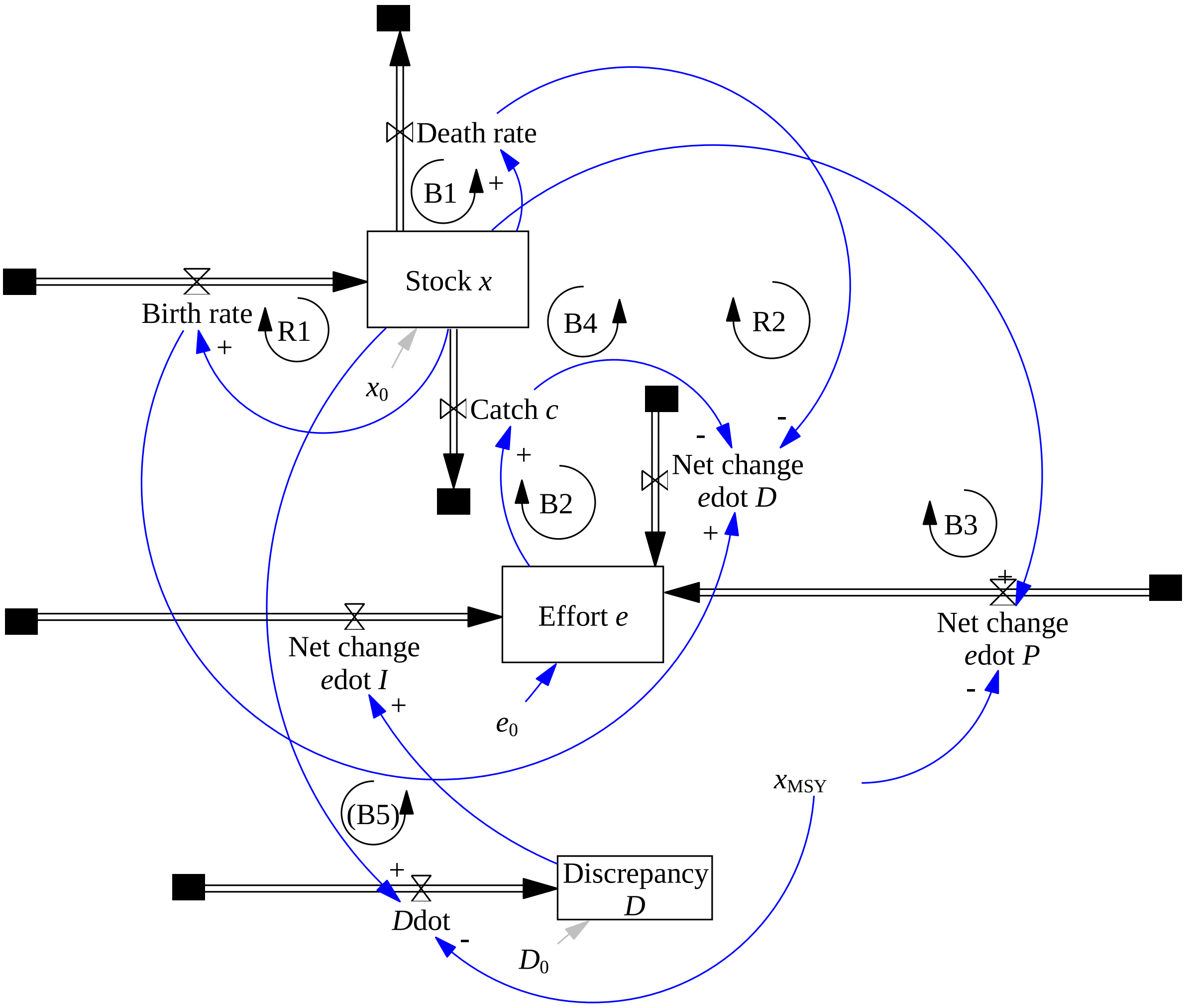


Figure 4 – The extensive stock and flow diagram of S-2 containing PID control

Table 6. Feedback loops in the extensive form of S-2

| No. | Order, sign | Loop |
|---|---|---|
| R1 | 1, + | Stock $x \xrightarrow{+}$ Birth rate $\xrightarrow{+}$ |
| B1 | 1, - | Stock $x \xrightarrow{+}$ Death rate $\xrightarrow{-}$ |
| B2 | 1, - | Effort $e \xrightarrow{+}$ Catch $c \xrightarrow{-}$ Net change edot $D$ |
| B3 | 2, - | Stock $x \xrightarrow{+}$ Net change edot $P \longrightarrow$ Effort $e \xrightarrow{+}$ Catch $c \xrightarrow{-}$ |
| R2 | 2, + | Stock $x \xrightarrow{+}$ Death rate $\xrightarrow{-}$ Net change edot $D \longrightarrow$ Effort $e \xrightarrow{+}$<br>$\xrightarrow{+}$ Catch $c \xrightarrow{-}$ |
| B4 | 2, - | Stock $x \xrightarrow{+}$ Birth rate $\xrightarrow{+}$<br>$\xrightarrow{+}$ Net change edot $D \longrightarrow$ Effort $e \xrightarrow{+}$ Catch $c \xrightarrow{-}$ |
| B5 | 3, - | Stock $x \xrightarrow{+}$ Ddot $\longrightarrow$ Discrepancy $D \xrightarrow{+}$<br>$\xrightarrow{+}$ Net chande edot $I \longrightarrow$ Effort $e \xrightarrow{+}$ Catch $c \xrightarrow{-}$ |

The intensive deterministic form of S-2 is the system of three ODEs – two non-linear (3) and (17) as well as one linear (18):

$$\dot{e} = \frac{k_1\left(x - x_s\right) + k_2 D + k_3 \dot{x}}{h} =$$

$$= \frac{k_1\left(x - x_s\right) + k_2 D + k_3 (x - x^2 - eh)}{h} \qquad (17)$$

$$\dot{D} = x - x_s, \qquad (18)$$

where $k_1 > 0,\ k_2 > 0, k_3 > 0.$

For this system the Jacobi matrix is defined as

$$J_{\text{S-2}} = \begin{array}{|c|c|c|} \hline 1 - 2x & -h & 0 \\ \hline \dfrac{k_1 + k_3(1-2x)}{h} & -k_3 & \dfrac{k_2}{h} \\ \hline 1 & 0 & 0 \\ \hline \end{array}. \qquad (19)$$

The reader sees S-2 can belong to predator (*e*) – prey (*x*) models whenever $\frac{\partial \dot{e}}{\partial x} > 0$ as $\frac{\partial \dot{x}}{\partial e} < 0$ is satisfied. There is predator intra-specific competition for $\frac{\partial \dot{e}}{\partial e} < 0$. Preys co-operate with each other if $x < 0.5$ and $\frac{\partial \dot{x}}{\partial x} > 0$ or compete with each other if $x > 0.5$ and $\frac{\partial \dot{x}}{\partial x} < 0$, a neutral case is for $x = x_s = 0.5$.

The above system has the non-trivial stationary state in the three-dimensional phase space:

$$F_s = (x_s, e_s, D_s). \qquad (20)$$

There are two differences between this stationary state $F_s$ and stationary state $E_s$ (8) in the two-dimensional phase space: first, at place of expected fitting sustainable effort $y_s$ there is fitting sustainable effort $e_s$ itself, second, only $F_s$ possesses the third component $D_s = 0$. The first component $x_s$ is common for the both stationary states.

Additionally this system has two trivial stationary states (0, 0, 0) and (1, 0, 0). The stability analyses of these two trivial stationary states on the phase plane are omitted for brevity.

For this system, i.e., ODEs (3), (17) and (18), the Jacoby matrix is defined as

$$J^*_{\text{S-2}} = \begin{array}{|c|c|c|} \hline 0 & -0.25 & 0 \\ \hline 4k_1 & -k_3 & 4k_2 \\ \hline 1 & 0 & 0 \\ \hline \end{array}. \qquad (21)$$

Figure 5 and Table 7 reflect the compact stock and flow diagram of the intensive form of S-2 near the stationary state $F_s$, a total number of feedback loops – 4, among them: 1st order – 2 (negative and *positive*), 2nd order – 1 (negative), 3rd order – 1 (negative).

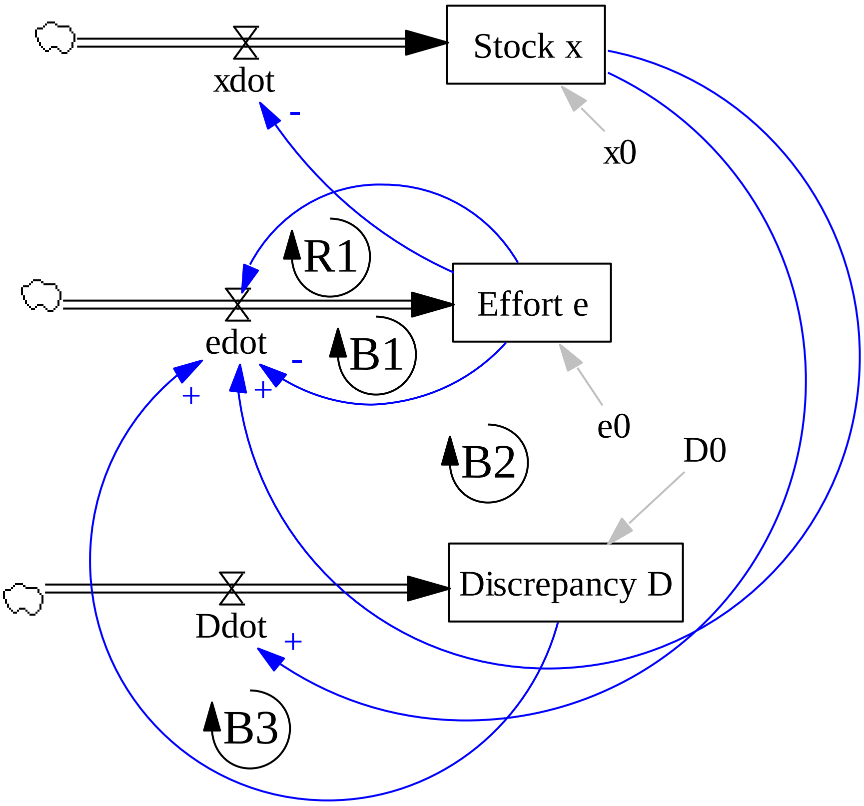


Figure 5 – The intensive SFD for a local vicinity of the stationary state $F_s$ in S-2

Table 7. Intensive feedback loops in S-2 at the stationary state $F_s$ in S-2

| No. | Order, sign | Loop |
|---|---|---|
| B1 | 1, - | $e \xrightarrow{-} \dot{e}$ if $\dot{e} < 0$ |
| R1 | 1, + | $e \xrightarrow{+} \dot{e}$ if $\dot{e} > 0$ |
| B2 | 2, - | $x \xrightarrow{+} \dot{e} \longrightarrow e \xrightarrow{-} \dot{x}$ |
| B3 | 3, - | $x \xrightarrow{+} \dot{D} \longrightarrow D \xrightarrow{+} \dot{e} \longrightarrow e \xrightarrow{-} \dot{x}$ |

The characteristic equation of the third order related to Jacobi matrix $J^{*}_{\text{S-2}}$ (21) is written as

$$\lambda^3 + a_2\lambda^2 + a_1\lambda + a_0 = 0, \tag{22}$$

where

$$a_0 = \quad k_2 > 0, \tag{23}$$

$$a_1 = k_1 > 0, \tag{24}$$

$$a_2 = k_3 > 0. \tag{25}$$

**Proposition 2** The dynamics of the system (3), (17) and (18) linearized in the neighbourhood of its hyperbolic stationary state $F_s$ (20) are LAS provided that $a_1a_2 > a_0$ or $0 < k_2 < k_1k_3$. Then stationary state $F_s$ is also LAS in the non-linear system (3), (17) and (18). Stationary state $F_s$ (20) is *not* stable for $k_2 \geq k_1k_3$ in the linearized system based on (3), (17) and (18).

The proof of Proposition 2 is easily maintained by the Routh–Hurwitz criterion thanks to lucidity of (23) – (25). We see each requirement of the Routh–Hurwitz criterion has the respective practical counterpart in PID control that realizes this criterion in real life. There is also the significant restriction on the relative “strength” of these requirements: the subordinate relation of $k_2$ to $k_1k_3$. The violation of this subordination is destabilizing.

**Proposition 3** For $k_2^{critical} = k_1k_3$, the characteristic equation is specified as

$$(\lambda^2 + k_1)(\lambda + k_3) = 0 \tag{26}$$

therefore

$$\lambda_1 = -k_3 < 0 \tag{27}$$

and

$$\lambda_{2,3} = \pm i\sqrt{k_1}\ . \tag{28}$$

The proof of Proposition 3 is easily derived for (22) with $k_2^{critical} = k_1k_3$.

**Proposition 4** For $k_2^{AHB} \approx k_2^{critical}$ and $k_2^{AHB} < k_2^{critical} = k_1k_3$, the Andronov – Hopf bifurcation (AHB) does take place in the system (3), (17) and (18) in a local vicinity of $F_s$ (20). Then, according to the Hopf theorem, there exists some periodic solution bifurcating from $F_s$ and the period of fluctuations is about

$$T_c \approx \frac{2\pi}{\sqrt{a_1}} = \frac{2\pi}{\sqrt{k_1}}\ . \tag{29}$$

The proof of Proposition 4 is omitted for brevity.

If a closed orbit is an attractor, it is called a *limit cycle*. The existence of limit cycle in S-2 has not been established. The Hopf theorem establishes only the existence of closed orbits in a neighbourhood of $F_s$ at $k_2^{critical}$, still it does not clarify the stability of orbits. Its edge-knife property is revealed by simulation experiments.

### 3.2 Loop tuning through parametric policy optimization

As known from the literature, loop tuning is the art of selecting values for tuning parameters that enable the controller to eliminate the error quickly without causing excessive process variable fluctuations [11].

The author has carried out PID loop tuning through policy optimization for the given LAS stationary state $F_s$. The optimization criterion is mostly grasped as a cumulative catch over 0–T years. Besides this, Penalty for negative effort $e$ is added in Pay-off:

$$\text{Penalty} = \int_0^T \delta dt \tag{30}$$

where $\delta = 0$, if $e \geq 0$, $\delta = -10^7$, if $e < 0$.

Formally, this policy optimization in Vensim is based on a restricted dynamic optimization problem, $T = 100$:

$$\text{Max}\left(0.1\int_0^T ehdt + 0.9\int_0^T \delta dt\right), \tag{31}$$

subject to (3), (17) and (18)
with $(x_0, e_0, D_0) = (0.4, 1, 0)$,

where initially:

$$0 \le k_2 = 0.102827 \le 0.5,$$
$$0 \le k_3 = 0.5 \le 15,$$
$$0.5 \le k_1 = 0.5 \le 5.$$

A quasi-optimal solution yields the parameters' magnitudes:

$$0 \le k_2 = 8.1087\text{e-}005 \approx 0 \le 0.5,$$
$$0 \le k_3 = 3.6256 \le 15,$$
$$0.5 \le k_1 = 5 \le 5.$$

Whereas the magnitude of $k_3$ is within the bounds, the magnitude of $k_1$ is at the right hand border of the selected segment, the magnitude of $k_2$ is practically zero at the left hand border of the respective segment.

Table 8 and Table 9 post information on two dynamic modes in S-2: the first mode is asymptotic convergence to the stationary state $F_s$, the second mode is entirely oscillatory around the same stationary state in the three-dimensional phase space for *x*, *e* and *D*. The difference of these two modes is rooted in particular magnitudes of parameter $k_2$ when other conditions remain the same.

Table 8. The roots of the characteristic equation (22) for the stable focus-node in S-2

| $k_2$ | $\lambda_1$ | $\mathrm{Re}(\lambda_2, \lambda_3)$ | $\mathrm{Im}(\lambda_2, \lambda_3)$ |
|---|---|---|---|
| 0.000081 | –0.000016 | –1.813 | ±1.309 |

Table 9. Roots of the characteristic equation (22) for Andronov – Hopf bifurcation in S-2

| Bifurcation | $k_2^{critical}$ | $\lambda_1$ | $\mathrm{Re}(\lambda_2, \lambda_3)$ | $\mathrm{Im}(\lambda_2, \lambda_3)$ | $k_2^{AHB}$ | Period of closed orbit |
|---|---|---|---|---|---|---|
| AHB | 18.128 | –3.626 | 0 | ±2.236 | 18.1 | 2.81 |

Figures 6–11 reflect the two delineated regimes of harvesting explained above (Propositions 2 and 3). Figures 12–15 relate to other significant bio-economic aspects of the runs carried out for S-2 and M-2 to be compared in next section.

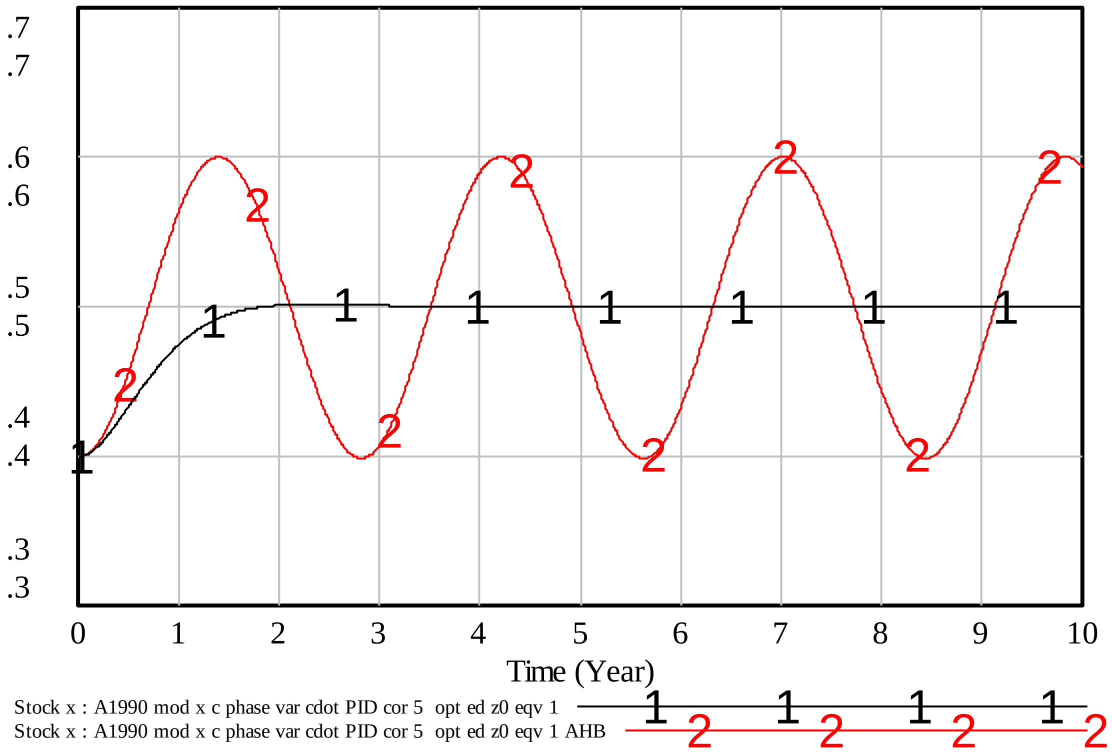


Figure 6 – Dynamics of stock *x*: transition to stationary magnitude (1) and movement along closed orbit (2) with the period of 2.81 y. in result of AHB, 0–10 years

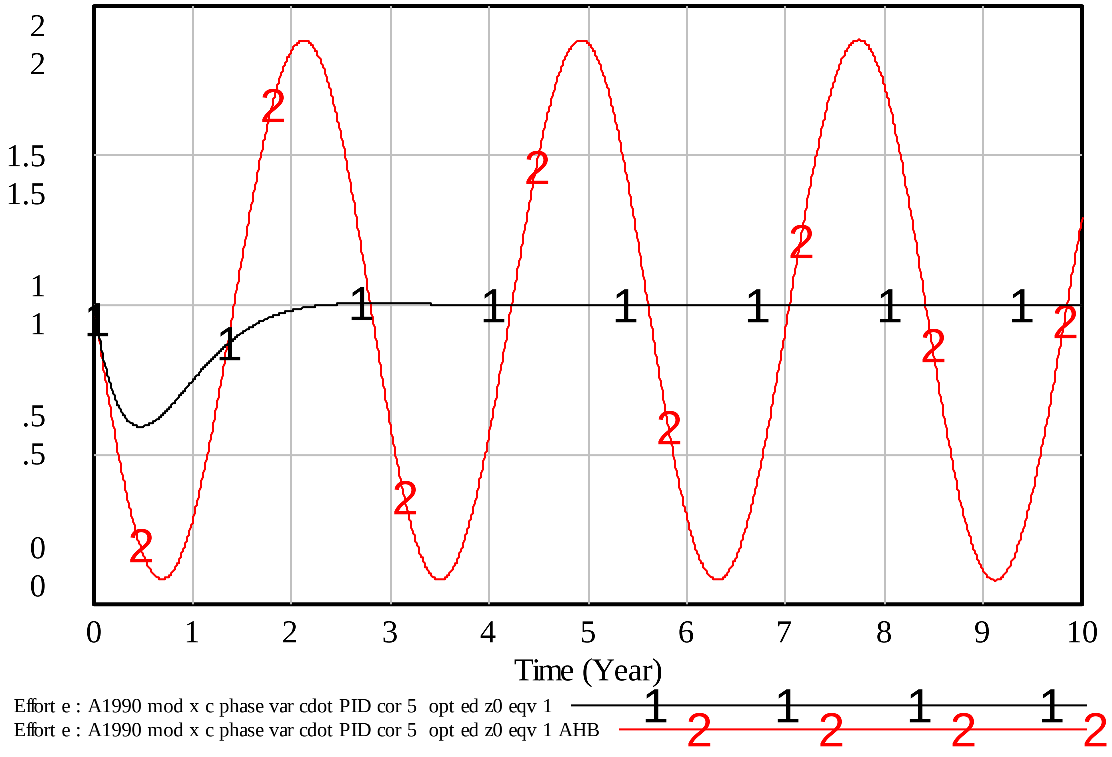


Figure 7 – Dynamics of effort *e*: transition to stationary magnitude (1) and movement along closed orbit (2) with the period of 2.81 y. in result of AHB, 0–10 years

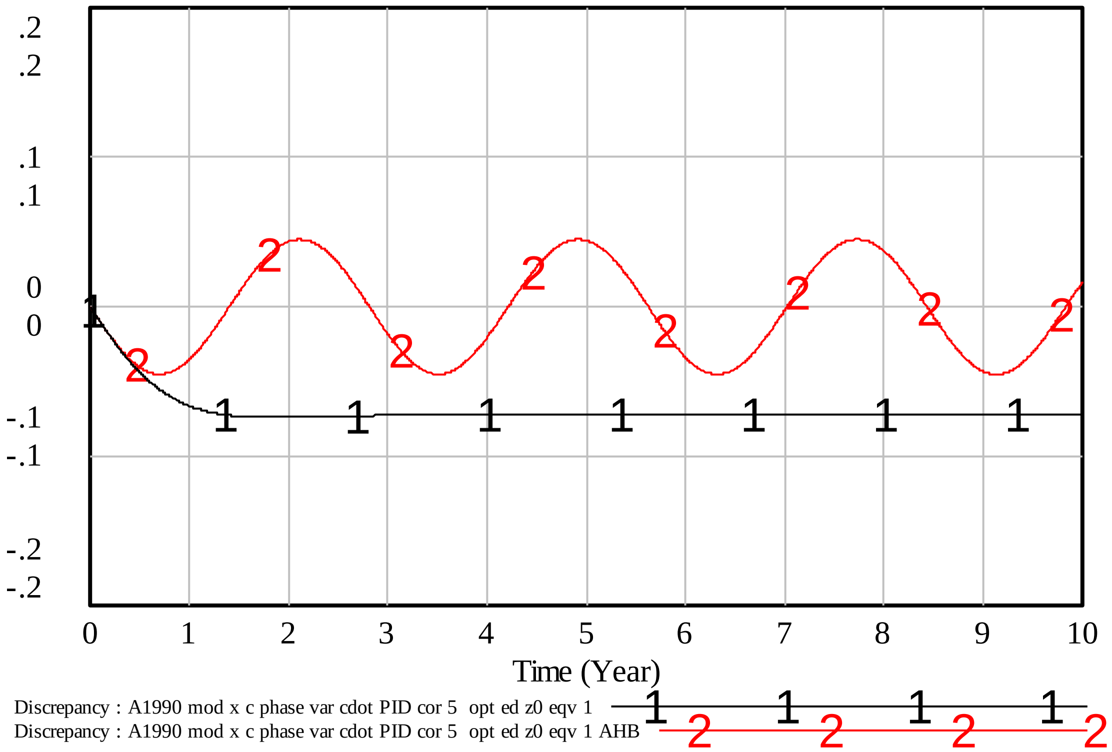


Figure 8 – Dynamics of Discrepancy *D*: transition to stationary magnitude (1) and movement along closed orbit (2) with the period of 2.81 y. in result of AHB, 0–10 years

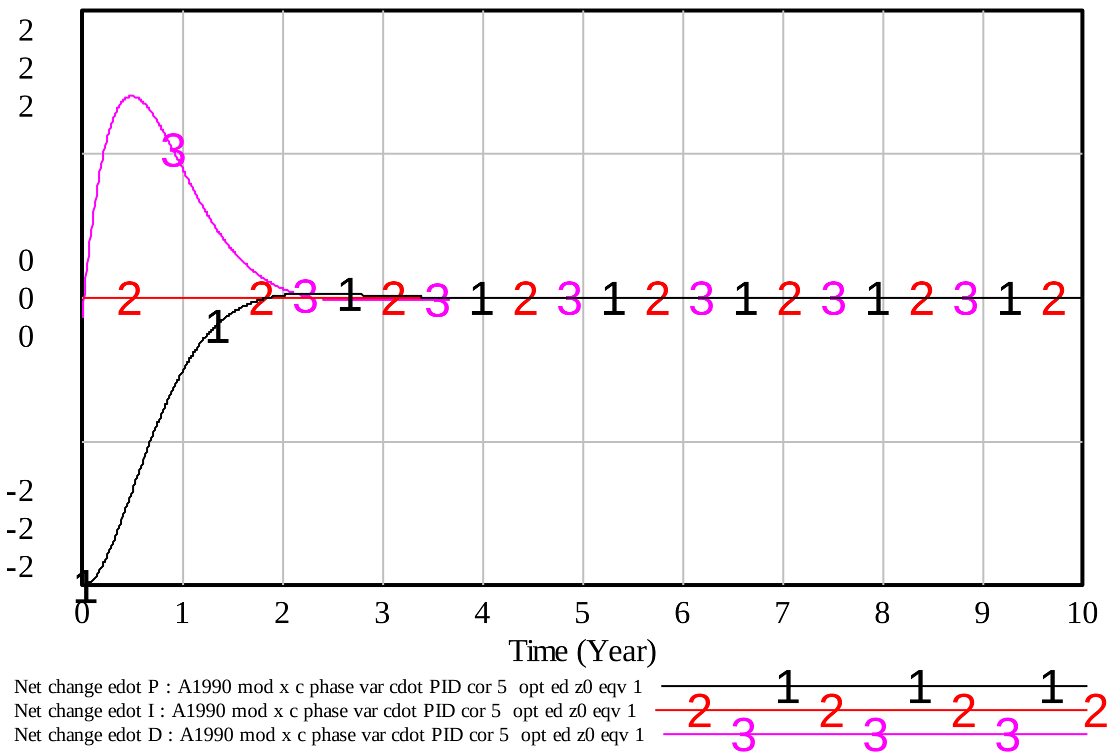


Figure 9 – Components of net change of catch *e*: (1) – proportional, (2) – integral, (3) – derivative for transition to the stationary state, 0–10 years

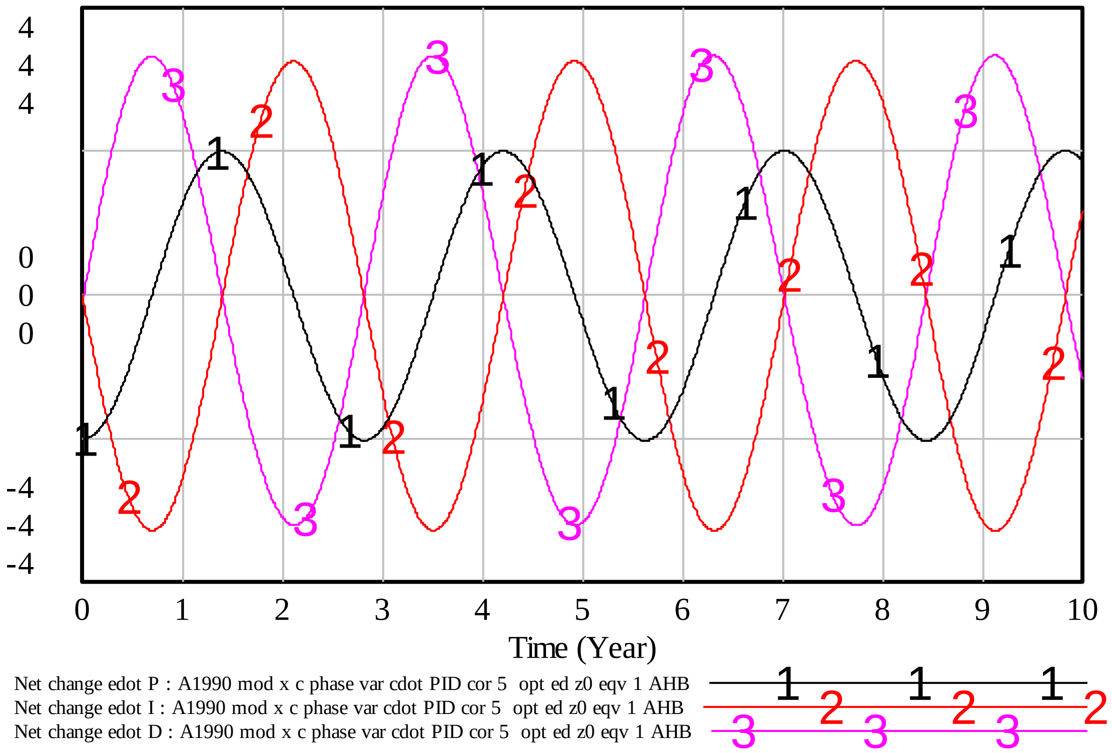


Figure 10 – Components of net change of catch *e*: (1) – proportional, (2) – integral, (3) – derivative for closed orbit with the period of 2.81 y. in result of AHB, 0–10 years

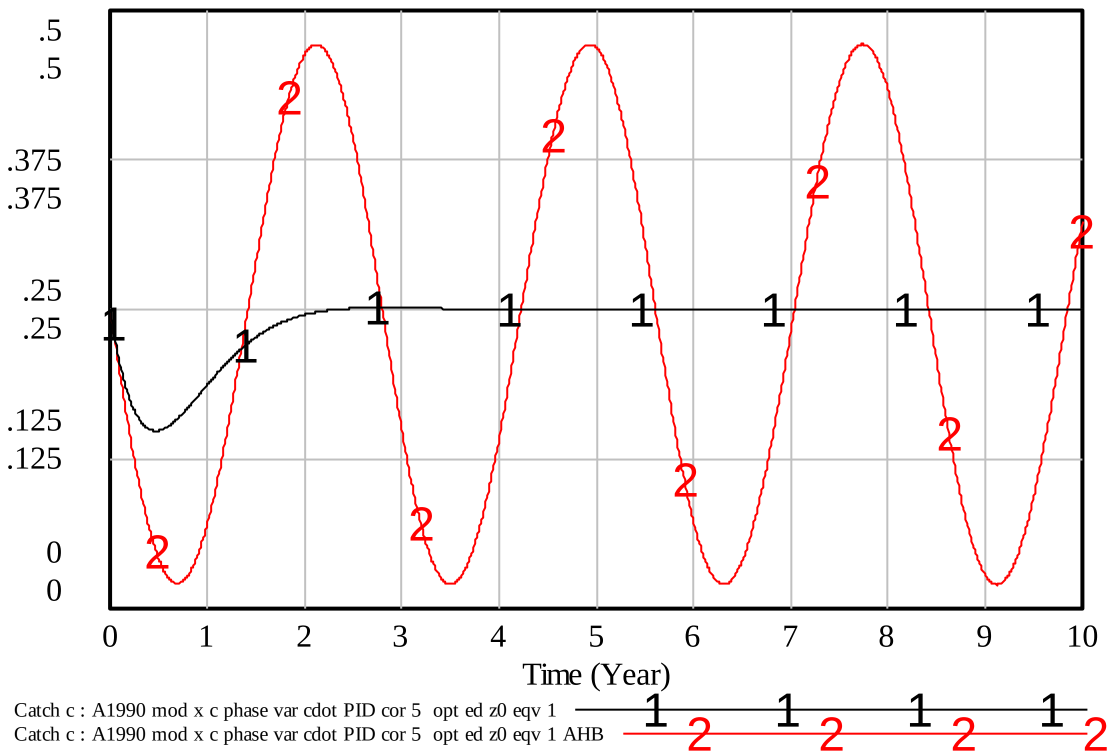


Figure 11 – Dynamics of catch *c*: transition to stationary magnitude (1) and movement along closed orbit (2) with the period of 2.81 y. in result of AHB, 0–10 years

## 4 Revealing correspondence of the harvesting control rules in M-2 and S-2

The author has carried out policy optimization for the given LAS $E_s$ in M-2 containing the heuristic HCR. The optimization criterion is mostly grasped as cumulative catch over 0–T years again. Besides this, Penalty for negative catch $c$ is added in Pay-off also:

$$\text{Penalty} = \int_0^T \delta dt \qquad (32)$$

where $\delta = 0$, if $c \geq 0$, $\delta = -10^7$, if $c < 0$.

Formally, this policy optimization in Vensim is based on a restricted dynamic optimization problem, $T = 100$:

$$\text{Max}\left(0.1\int_0^T ehdt + 0.9\int_0^T \delta dt\right), \qquad (33)$$

subject to (3) and (6)

with $(x_0, y_0) = (0.4, 1.25)$,

where initially

$$e_0 = 1,$$
$$0 \leq \alpha = 0.9 \leq 1 \text{ and}$$
$$1 \leq AdjT = 10 \leq 25.$$

A quasi-optimal solution yields the parameters' magnitudes: $\alpha = 1$ and $AdjT = 1.21635$. The magnitude of $\alpha$ is at the right hand border of the appropriate segment, the magnitude of $AdjT$ is within bounds of the respective segment still it is much lower than $AdjT = 10$ in [13, p. 152].

Before presenting details of the optimization run in M-2 let us consider the correspondence of HCLs in M-2 and S-2.

**Proposition 5** It is possible for PID control in S-2 to match the heuristic HCR in M-2 even with inactive integral element when $k_2 = 0$.

***Proof of Proposition 5*** Compare the Jacoby matrix for characteristic equation (10) for M-2 and the fragment of the Jacoby matrix for characteristic equation (22) for S-2 (Table 10).

Table 10. Comparison of the fragment of Jacoby matrix $J^*_{S\text{-}2}$ with the Jacoby matrix $J^*_{M\text{-}2}$

| $J^*_{S\text{-}2}$ | | $J^*_{M\text{-}2}$ | |
|---|---|---|---|
| 0 | –0.25 | $-0.5\alpha < 0$ | $-0.25 < 0$ |
| $4k_1 > 0$ | $-k_3$ | $2d\alpha > 0$ | 0 |

Almost perfect matching of linear proportional and derivative (PD) control over $x$ and $e$ without active integral element in 3-dimentional S-2 and nonlinear proportional and derivative (PD) control in 2-dimentional M-2 is achieved for the same initial conditions $x_0$ and $e_0$ with over-exploited fish stock when the congruity conditions are satisfied:

$$k_1 = 0.5d\alpha, \qquad (34)$$
$$k_2 = 0, \qquad (35)$$
$$k_3 = 0.5\alpha. \qquad (36)$$

The match between S-2 with the appropriate magnitudes of the three control parameters and M-2 with corresponding quasi-optimal magnitudes of the two control parameters is achieved for $k_1 = 0.5d\alpha = 0.41105$, $k_3 = 0.5\alpha = 0.5$, $k_2 = 0$. Table 11 provides additional details of congruity between these specifications. In both models, there is a converging cycle with period of 10.642 y.

Table 11. Matching characteristics for optimization run in M-2 and congruent run in S-2

| Root | Characteristics for LAS focus $F_s$ in S-2 | Characteristics for LAS focus $E_s$ in M-2 |
|---|---|---|
| $\lambda_3$ | 0 | - |
| $\mathrm{Re}(\lambda_1)$ | –0.25 | –0.25 |
| $\mathrm{Im}(\lambda_1)$ | 0.59039$i$ | 0.59039$i$ |
| $\mathrm{Re}(\lambda_2)$ | –0.25 | –0.25 |
| $\mathrm{Im}(\lambda_2)$ | –0.59039$i$ | –0.59039$i$ |
| Period $T_c$ | 10.64234 y. | 10.64234 y. |

The congruent run in S-2 has a slightly higher (measured by a few hair width) bio-economic efficiency than the quasi-optimal run in M-2. Distinctly, the mostly efficient is the quasi-optimal run in S-2 (see Figures 12–15 and Table 12).

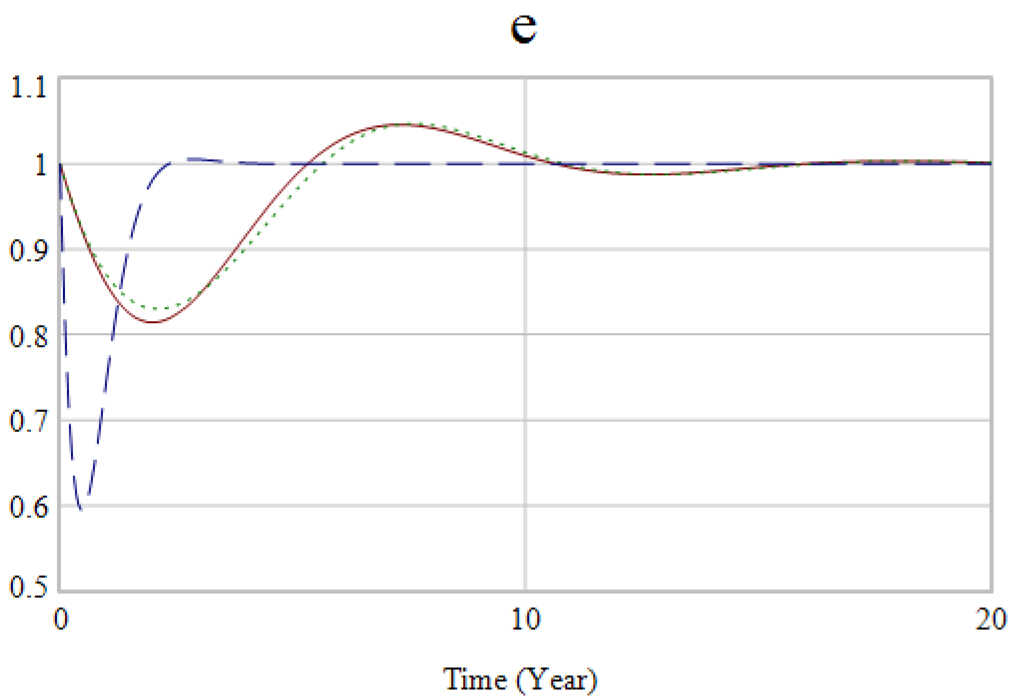


Figure 12 – Transition of effort $e$ to fitting sustainable effort $e_s = 1$; solid curve – congruent run in S-2, dotted curve – quasi-optimal run in M-2, piece-wise curve – quasi-optimal run in S-2, 0–20 years

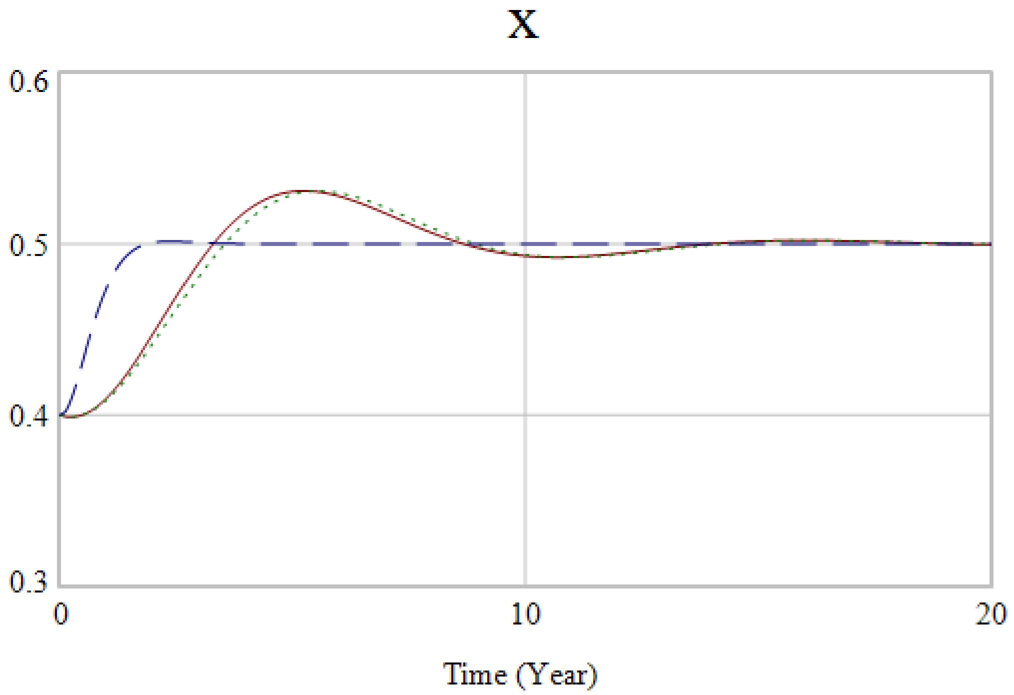


Figure 13 – Transition of stock $x$ to sustainable $x_s = 0.5$; solid curve – congruent run in S-2, dotted curve – quasi-optimal run in M-2, piece-wise curve – quasi-optimal run in S-2, 0–20 years

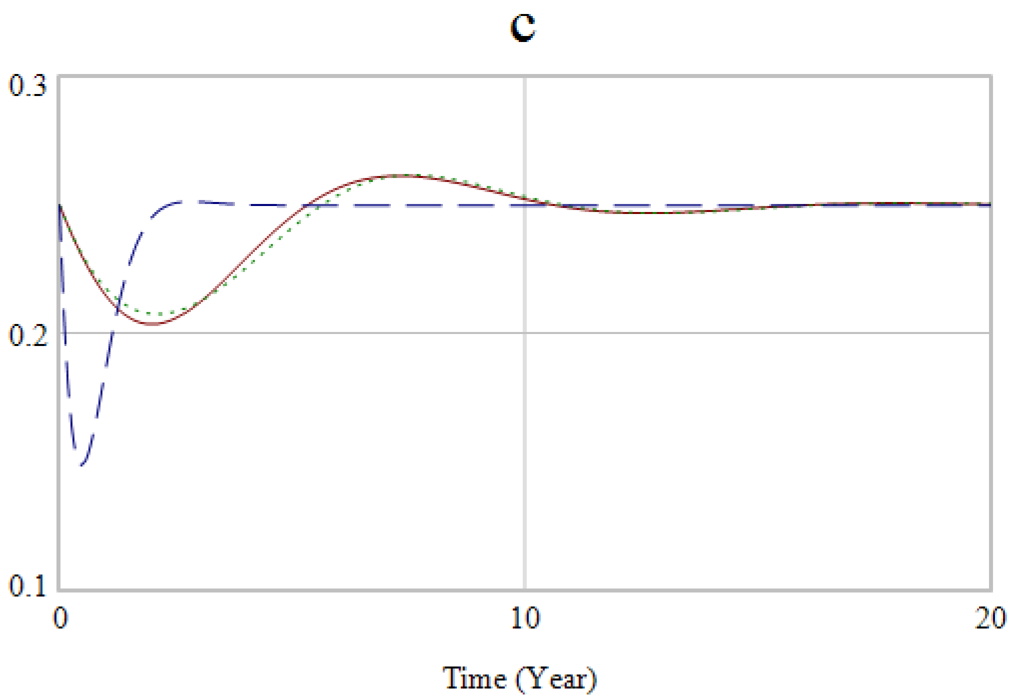


Figure 14 – Transition of catch $c$ to maximal sustainable yield $c_s = 0.25$; solid curve – congruent run in S-2, dotted curve – quasi-optimal run in M-2, piece-wise curve – quasi-optimal run in S-2, 0–20 years

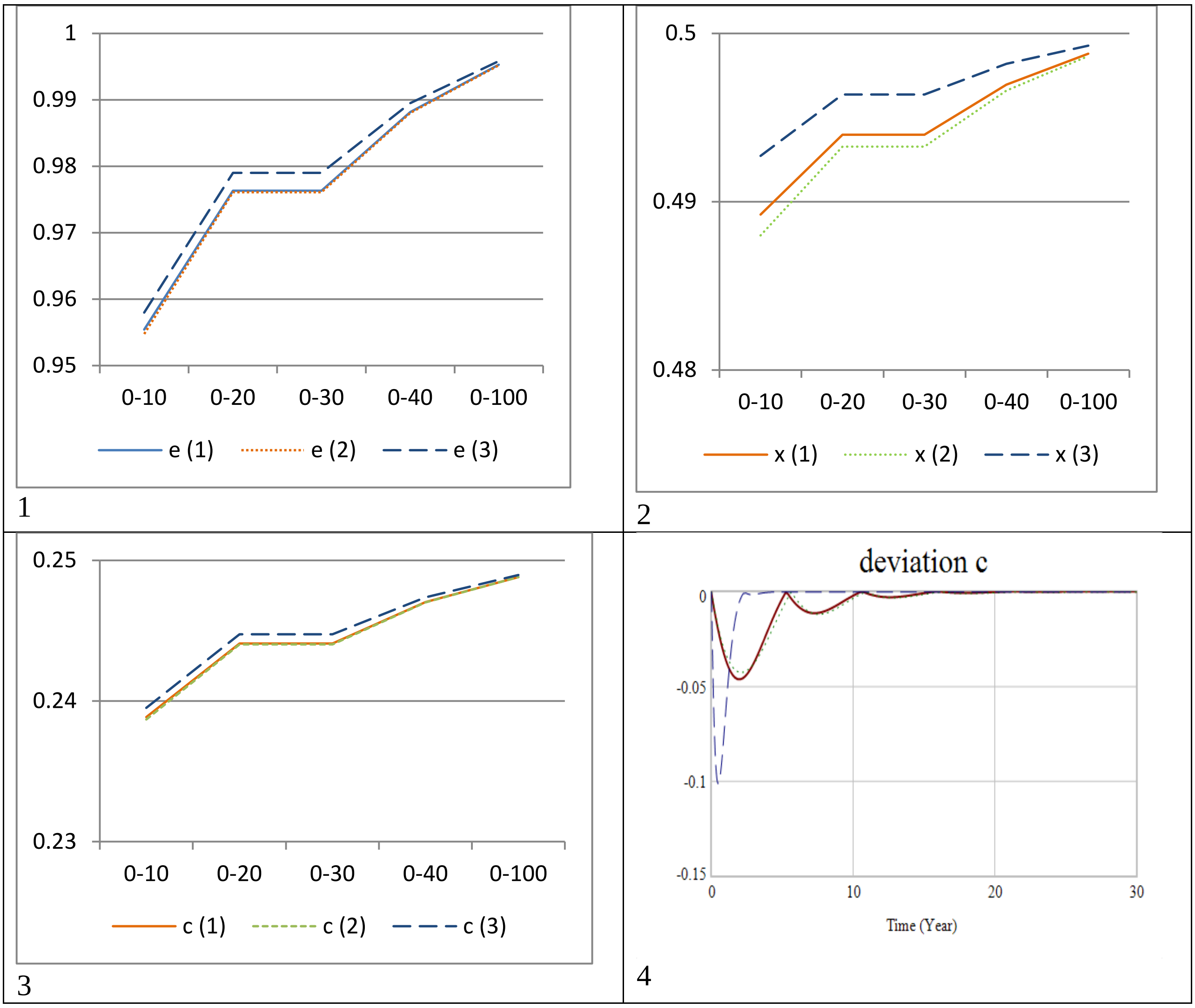


Figure 15 – Evolution of average magnitudes over decades; panel 1 – effort *e*, panel 2 – fish stock *x*, panel 3 – catch *c*, 0–100 years and panel 4 – real-time deviation of catch *c* from MSY $c_s$, 0–30 years; (1) solid curve – congruent run in S-2, (2) dotted curve – quasi-optimal run in M-2, (3) piece-wise curve – quasi-optimal run in S-2

Table 12. Absolute and relative deviations of average magnitudes from target magnitudes ($x_s$ =0.5 for *x*, $e_s$ = 1 for *e* and $c_s$ =0.25 for *c*) in the three runs over 0–100

| Run | Absolute deviation | Relative deviation. % |
|---|---|---|
| | Stock *x* | |
| (1) – congruent in S-2 | –0.0012 | –0.244 |
| (2) – quasi-optimal in M-2 | –0.0014 | –0.272 |
| (3) – quasi-optimal in S-2 | –0.0007 | –0.146 |
| | Effort *e* | |
| (1) – congruent in S-2 | –0.0048 | –0.475 |
| (2) – quasi-optimal in M-2 | –0.0048 | –0.481 |
| (3) – quasi-optimal in S-2 | –0.0042 | –0.421 |
| | Catch *c* | |
| (1) – congruent in S-2 | –0.0012 | –0.476 |
| (2) – quasi-optimal in M-2 | –0.0012 | –0.48 |
| (3) – quasi-optimal in S-2 | –0.0011 | –0.42 |

**Proposition 6** It is not always possible to match PID control in S-2 through the heuristic HCR in M-2. Therefore PID control in S-2 generalizes the heuristic HCR in M-2.

***Proof of Proposition 6*** The integral control element is absent in M-2 with the heuristic HCR. Even when the integral control element is not active in S-2, matching the heuristic HCR in M-2 is not always possible.

The counter-example serves as the decisive argument. Take the magnitudes from quasi-optimal run in S-2: $k_1 = 5$ and $k_3 = 3.6256$. The attempted congruity would require $\alpha = 2k_3 = 7.2512 >> 1$, $d = 1.3791$, $AdjT = 1/d = 0.72512$, $y_0 = -2.221 < 0$. These magnitudes of the control parameters are not possible in M-2. Next assertion is the crown of the present research.

**Proposition 7** PID control in S-2 is a generalization of the heuristic HCR in M-2.

***Proof of Proposition 7*** Put Propositions 5 and 6 together and claim their synthesis.

PID control in S-2 is generalization for the heuristic HCR in M-2. The new experimental material shows that PID control provides optimal (or close to optimal) HCR either when the heuristic HCR does this or when it does not.

## *Conclusion*

One of the strengths inherent in the method of system dynamics is to account for the impacts of alternative hypotheses on the behaviour of the complete system using systems of equations. This paper provides new experimental and analytical material to substantiate this strength of the system dynamics method (still under only deterministic conditions so far).

Typical modes of renewable resource management are considered for closed-loop control. Using the mathematic control theory, the policies of improving bio-resources catch and renewal, with raised long-term effectiveness in relation to the policy proposed in the simplified Verhulst – Schaefer bio-economic model M-2 with the heuristic HCR are elaborated in S-2 that applies proportional, derivative and integral (PID) control.

The obtained results related to the compared bio-economic modes (regimes) are not only local, as is often the case in the applications of catastrophe theory, but also global in nature (particularly, in S-2 with PID control that is effective and efficient even far from equilibrium). For all the considered modes (regimes) in two- and three-dimensional models, the differential, integral and auxiliary equations are derived. Still the analytical results for the proposed two- and three-dimensional predator-prey models M-2 and S-2 are mostly local; they are extended to broader areas (spaces) thanks to Vensim simulations.

This paper substitutes the heuristic harvesting control rule (HCR) by the original HCR based on the standardised PID control. This heuristic HCR is essentially a special case of this PID control. The congruent run in S-2 is slightly better than the quasi-optimal run in M-2; the quasi-optimal run in S-2 is the best among these three distinctly. It would be interesting to augment the heuristic HCR by an integral element of control as well.

The effective and efficient PID control can be reduced to similar PD control under variety of settings. The over-extended integral element of control is destabilizing and tends to create oscillations that can be converging, steady or diverging depending on the parameters' constellations and on initial magnitudes of the fish stock.

The author intends to raise the dimension of the two main models through information delays in the measurement of the fish stock in decision-making. Obtaining knowledge of a critical delay length could facilitate the PID control further.

A more concrete presentation of the ecological and economic reproduction and its current global crisis is expected to be carried out in further studies with detailed elaboration of technological and institutional aspects.

The transition from the above simplified aggregated analysis of sustainability to the study of the evolutionary ecological stability of interacting bio-resources is promising [18]. Besides disaggregation of bio-mass into specific components in different geographical regions, the research should also enhance the probabilistic approach to bio-economic modelling.

## *References*

1. Clark C. 1990. Mathematical Bioeconomics: The Optimal Management of Renewable Resources. 2nd ed. New York: John Wiley & Sons.

2. Whelan J., G., Diamond A. 1994, 2001. Building the Fish Banks Model and Renewable Resource Depletion // Working Paper D-4543-2. Sloan School of Management (MIT).

3. World Bank and FAO. 2009. The Sunken Billions: The Economic Justification for Fisheries Reform. Washington, DC: World Bank. – 100 p. URL: https://openknowledge.worldbank.org/bitstream/handle/10986/2596/476060PUB0Sunk101Official0Use0Only1.pdf?sequence=1&isAllowed=y

4. World Bank. 2017. The Sunken Billions Revisited. Progress and Challenges in Global Marine Fisheries. Washington, DC: World Bank. – 99 p.
URL: https://openknowledge.worldbank.org/handle/10986/24056

5. FAO. 2022. The State of World Fisheries and Aquaculture 2022. Towards Blue Transformation. Rome, FAO. URL: https://doi.org/10.4060/cc0461en

6. Emel'yanov S. V., Burovoi I. A., Levada F. Yu. (Eds.) 1998. Control of Indefinite Nonlinear dynamic systems. Induced internal feedback // Lecture Notes in Control and Information Sciences, 231, Springer, 1998.

7. Intriligator M.D. 2002. Mathematical Optimization and Economic Theory. SIAM. – 529 p. – (Classics in Applied Mathematics).

8. Ryzhenkov A.V. 2015. An Enhancement for the textbook's models of natural resources and economic growth // The 33rd International Conference of the System Dynamics Society "Reinventing Life on a Shrinking Earth", Cambridge, Massachusetts, USA. July 19 – July 23, 2015 [Electronic resource]. – Cambridge, 2015. – Economics. –
Abstract URL: http://www.systemdynamics.org/web.portal?A1366+0
Paper URL: http://www.systemdynamics.org/web.portal?P1366+0
Supporting URL: http://www.systemdynamics.org/web.portal?S1366+0

9. Ryzhenkov A.V. 2018. Shedding light on the harvesting control rules in abstract bioeconomic models // The 36th International Conference of the System Dynamics Society. Reykjavik, Iceland.
URL: http://proceedings.systemdynamics.org/2018/proceed/papers/P2297.pdf

10. Ryzhenkov A.V. Controlling effort, catch and biomass in models of the global marine fisheries. – DOI: 10.1088/1742-6596/2092/1/012021 // IOP Conference Series: Journal of Physics: Conference Series : Eleventh International Scientific Conference and Young Scientist

School "Theory and Computational Methods for Inverse and Ill-posed Problems" 26 August - 4 September 2019, Novosibirsk, Russia. – 2021. – Vol. 2092. – Article Number 012021. Scopus. – URL: https://iopscience.iop.org/article/10.1088/1742-6596/2092/1/012021 (Published online: 20 December 2021).

11. Bansal H., Sharma R., Shreeraman R. 2012. PID controller tuning techniques: a review // Journal of Control Engineering and Technology (JCET) 2 (4): 168–176.

12. Schaefer M.B. 1954. Some aspects of the dynamics of populations important to the management of commercial marine fisheries // Bulletin of Mathematical Biology 53 (1/2): 253–279, 1991 ed., 1 (2): 27–56.

13. Moxnes E 2004 (Summer) Misperceptions of basic dynamics: the case of renewable resource management // System Dynamics Review Vol. 20, No. 2: 139–162

14. Gandolfo G. 2010. *Economic dynamics*. Heidelberg: Springer.

15. Kuznetsov Y. A. 1998. Elements of Applied Bifurcation Theory (Second ed.). Berlin a.o.: Springer. ISBN 0-387-98382-1.

16. Arnold V. I. 1990. Catastrophe Theory. 3rd ed. Moscow, Nauka.

17. Araki M. "PID Control". URL: http://www.eolss.net/ebooks/Sample%20Chapters/C18/E6-43-03-0 Accessed March 12 2022.

18. Van den Bergh J. 2007. Evolutionary thinking in environmental economics // Journal of Evolutionary Economics 17: 521–549.

## Acknowledgements

The author is grateful for the reviewers of the submitted manuscript for their critical remarks and appreciates generous efforts of the ISDC-2022 organizers.

This study has been carried out with the plan of research work of IEIE SB RAS; base project "Methods and models for substantiating the strategy for the development of the Russian economy in the context of a changing macroeconomic reality", no. 5.6.6.4. (0260-2021-0008).